Estimates of EAST Operation Window with LHCD by Using a Core-SOL-Divertor Model

2014 Plasma Sci. Technol. 16 907

(http://iopscience.iop.org/1009-0630/16/10/02)

Estimates of EAST Operation Window with LHCD by Using a Core-SOL-Divertor Model*

OU Jing (欧靖)[1,2], GAN Chunyun (甘春芸)[1], YE Lei (叶磊)[1]

[1]Institute of Plasma Physics, Chinese Academy of Sciences, Hefei 230031, China
[2]Center for Magnetic Fusion Theory, Chinese Academy of Sciences, Hefei 230031, China

Abstract An experimental advanced superconducting tokamak (EAST) operation window with the lower hybrid current drive (LHCD) in H-mode is estimated by using a core-SOL-divertor (C-S-D) model validated by the present EAST divertor experiments. The operation window consists of four limits including two usual limits, one of which is the maximum allowable heat load onto the divertor plate, and two additional limits associated with the LHCD. The predictive EAST operation window is not qualified to fulfill its mission for high input power. To extend the operation window, gas puffing and impurity seeding are presented as two effective methods. In addition, the effect of the LHCD current on the operation window is also discussed. Our numerical analysis results provide a reference for the safe operation of EAST experiments with LHCD in future.

Keywords: operation window, C-S-D model, numerical analysis

PACS: *52.55.Fa, 52.40.Hf, 52.55.Rk*

DOI: 10.1088/1009-0630/16/10/02

(Some figures may appear in colour only in the online journal)

1 Introduction

In tokamak scrape-off layer (SOL) region, a significant part of the heating power across the separatrix is transported primarily along magnetic field lines to the divertor target. At the divertor target, it must be reduced below a technologically feasible value. For the high-powered steady-state tokamak devices such as EAST, power handing is a critical issue in the long pulse operation. To ensure the energy flux to the target plate below the engineering design maximum, before EAST operation, predictive analysis of divertor plasma performance has been investigated by the B2-Eirene code and two-point model [1−3]. Later, the estimated operation window was obtained by a simple C-S-D model [4,5]. However, in this C-S-D model, the particle flux and the heat flux across the separatrix, which are difficult to control or not obtained directly in the experiments, were used as the input control parameters. After April 2009 in EAST experiments, H-mode plasma was obtained with LHCD and several strategies are employed to reduce the energy flux load onto the target plate [6−10]. Based on the present EAST divertor experiment databases and the auxiliary heating system upgrade including the LHCD, the H-mode operation window for EAST must be re-estimated and the extended operation window should be explored due to the increase in the input heating power. In this paper, following Refs. [4,5], we develop a C-S-D model validated by the present EAST divertor experiments. Then, we use this model to estimate the EAST operation window with the LHCD by a systematic variation of line average density and input power.

2 C-S-D model

The operation window in tokamaks has been widely investigated with edge plasma simulations. Recently, based on the consistency between the edge plasma operation and the core plasma operation, C-S-D plasma simulation has been developed in some tokamaks, such as the international thermonuclear experimental reactor (ITER) [4,5,11,12]. There are several combination methods to construct a C-S-D model with the core plasma transport model and the edge plasma transport model [4,5,11−13]. In this paper, to estimate the EAST operation window with the LHCD, we construct a C-S-D model which consists of a zero-dimensional plasma model for the core plasma and a two-point plasma model for the SOL-divertor plasma. The C-S-D model is not sufficient to study detailed structures of the consistency between the core plasma operation and the edge plasma operation. However, it is very useful to understand qualitatively the possible operation window, especially, in the wide-range parameters space of

*supported by National Natural Science Foundation of China (Nos. 11105176 and 11105224)

input heating power and plasma density.

2.1 Core plasma model

There is a combination of neoclassical and anomalous core plasma transport in the one-dimensional (1-D) or 1.5-D model [14]. However, when one roughly estimates the operation region in a tokamak for plasma parameters, the 0-D plasma model based on ITER physics guidelines can be applied to the core plasma transport. In the 0-D model, the global power and particle balance are [15]

$$\frac{\mathrm{d}W_\mathrm{p}}{\mathrm{d}t} = -\frac{W_\mathrm{p}}{\tau_\mathrm{E}} + P_\mathrm{OH} + P_\mathrm{aux} - P_\mathrm{Loss}, \tag{1}$$

$$\frac{\mathrm{d}n}{\mathrm{d}t} = -\frac{n}{\tau_\mathrm{p}} + S, \tag{2}$$

where W_p and n denote the stored plasma thermal energy and plasma density. τ_E and τ_p are the energy confinement time and particle confinement time. S is the particle source term. P_OH, P_aux and P_loss are the total powers of Ohmic heating, auxiliary heating and the lost energy including the bremsstrahlung loss and synchrotron radiation loss, respectively. In EAST, P_aux includes the neutral beam injection (NBI), the ion cyclotron range of frequency (ICRF) heating, and the electron cyclotron range of frequency (ECRF) heating and the LHCD. For the LHCD, a 2.45 GHz LHCD system with a power output of 2 MW is available, and 4 MW is expected in the near future. The power of the LHCD is estimated by the following definition [4,5]

$$P_\mathrm{LHCD} = \frac{R\ln\Lambda I_\mathrm{LHCD} < n >_{20}}{0.122(j^*/p^*) < T >} \quad , \tag{3}$$

with R the major radii in m, I_LHCD the LHCD driven current in MA, $< n >_{20}$ the line average electron density in 10^{20} m^{-3}, and $< T >$ the core plasma temperature in eV. The assumption of $(j^*/p^*) = 10$ is adopted in the present paper. During the LHCD, a low density operation is usually preferable for the current drive efficiency and the resulting $< n >< 6.0 \times 10^{19}$ m^{-3} is required, though EAST can be able to run safely with $< n >= 1.0 \times 10^{20}$ m^{-3} in Ohmic discharges according to the Greenwald limit. However, recently, a new assessment method of Frascati Tokamak Upgrade (FTU) for the LHCD at high plasma density indicated that a higher electron temperature of the plasma edge and periphery would diminish parasitic non-linear wave-plasma effects that prevent the penetration of the coupled radio frequency power to the core [16].

From the particle and power balance of the core plasma, the total particle flux Γ_sep and the total heat flux Q_sep across the separatrix to the SOL can be written as $\Gamma_\mathrm{sep} = (< n > V_\mathrm{p})/\tau_\mathrm{p}$ and $Q_\mathrm{sep} = (0.048 < n >< T > V_\mathrm{p})/\tau_\mathrm{E}$ with V_p the plasma volume in m^{-3} [4,5,15]. For the core plasma in H-mode, the power across the separatrix to the SOL must exceed the H-L back transition threshold by a reasonable margin. To examine the consistency between the H-mode and SOL condition, the experimental scaling law of the L-H transition condition is applied to EAST as follows [17]

$$p_\mathrm{thr}(\mathrm{MW}) \geq 0.0488 < n >_{20}^{0.72} B_\mathrm{T}^{0.80} S_\mathrm{A}^{0.94}, \tag{4}$$

where, B_T is the toroidal magnetic field in T and S_A is the plasma surface area in m^2. EAST experimental results show that H-mode plasma was achieved when the input power exceeded the above L-H transition condition [8−10]. According to Eq. (4), the core plasma may stay in H-mode for low $< n >$, but the operation window for the case of $< n >< 1.0 \times 10^{19}$ m^{-3} is not considered in this paper since in the present EAST experiments, $< n >\geq 1.0 \times 10^{19}$ m^{-3} [6−10].

2.2 SOL-Divertor plasma model

In the SOL-divertor region, a general fluid description of plasma with one ion-species includes 2-D models such as B2-EIRINE [1,2,18], the 1-D model [19] and two-point model [3−5]. Since its results agree fairly well with the results of experiments and complicated numerical simulations, and in view of its clear physical concept and simple mathematic form, the Two-point model has been used widely to explain the results of the SOL-divertor experiments [20] and to survey the parameters for the operational region of the SOL-Divertor plasma for ITER and other reactor designs [3−5,21]. The basic equations in the two-point model include the pressure balance equation, the energy balance equation and the thermal conduction equation, as described below [3−5,20,21]:

$$f_\mathrm{mom} n_\mathrm{u} T_\mathrm{u} = 2 n_\mathrm{T} T_\mathrm{T}, \tag{5}$$

$$(1 - f_\mathrm{imp}) L_\mathrm{s} q_\perp = \Gamma_\mathrm{T} \lambda_\mathrm{E} \{\varepsilon + [\gamma + \frac{3}{2}(\frac{1}{\alpha} - 1)] T_\mathrm{T}\}, \tag{6}$$

$$q_\perp (1 - f_\mathrm{imp}) L_\mathrm{s}^2 = \frac{2\kappa_0 \lambda_\mathrm{E}}{7} (T_\mathrm{u}^{7/2} - T_\mathrm{T}^{7/2}). \tag{7}$$

where, the subscript 'u' and 'T' express the upstream SOL and divertor target region, respectively. L_s, $q_\perp$, Γ_T, λ_E and κ_0 are the connection length, energy flux from the core region, particle flux, radial energy decay length and electron heat conductivity, respectively. The coefficients f_mom and f_imp are the fractions of momentum loss and impurity radiation loss. $f_\mathrm{mom} = 1 - 2(\frac{\alpha}{\alpha+1})^{(\alpha+1)/2}$ where $\alpha = \frac{<\sigma v>_\mathrm{ion}}{<\sigma v>_\mathrm{ion} + <\sigma v>_\mathrm{cex}}$ is defined by the ionization cross section $< \sigma v >_\mathrm{ion}$ and charge cross section $< \sigma v >_\mathrm{cex}$ [20]. In Eq. (6), the coefficient $\gamma\,(\sim 7.0)$ is the sheath energy transmission coefficient. The heat load $\varepsilon\,(\sim 21.8$ eV) on the target plate comes from the recombination and radiation process, and the term $\frac{3}{2}(\frac{1}{\alpha} - 1) T_\mathrm{T}$ comes from the plasma-neutral charge exchange.

Since the characteristic time scale of the core plasma (of the order of 100 s) is much longer than that of SOL-divertor plasma (ms), the two-point model under steady state conditions can be coupled with a time dependent core transport model. To couple the core and

edge plasma model, the particle balance condition for the SOL-divertor regions plasma is used.

$$\Gamma_{\rm sep}S_{\rm A} + f_{\rm ion}^{\rm S-D}N_{\rm n} = \Gamma_{\rm T}2\pi R\lambda_\Gamma \sin\varphi, \quad (8)$$

where $f_{\rm ion}^{\rm S-D}$ is the ionization fraction in the divertor and SOL regions, $N_{\rm n}$ is the total neutral source in the edge region, λ_Γ is the radial particle flux decay length and φ is the angle of a magnetic field to the divertor target. With the assumption of all neutral particles originating at the divertor plate due to the plasma particle flux to the divertor target and gas puffing, $N_{\rm n}$ can be described as

$$N_{\rm n} = \Gamma_{\rm T}2\pi R\lambda_\Gamma \sin\varphi + N_{\rm puff}. \quad (9)$$

The coefficient $f_{\rm ion}^{\rm S-D}$ in the divertor and the SOL regions is defined by [4,5]

$$f_{\rm ion}^{\rm D} = 1 - \exp(-\frac{L_{\rm d}\sin\varphi}{\lambda_{\rm ion}^{\rm div}}), \quad (10)$$

and

$$f_{\rm ion}^{\rm S} = \frac{A_{\rm SOL}}{A_{\rm Core} + A_{\rm SOL}}, \quad (11)$$

where $\lambda_{\rm ion}^{\rm div} = v_{\rm n}/(n_{\rm T} < \sigma v >_{\rm ion})$ is the neutral penetration length associated with neutral velocity $v_{\rm n} = \sqrt{T_{\rm n}/m}$ with the assumption of neutral temperature $T_{\rm n} = T_{\rm T}$. $A_{\rm SOL} = 2\pi R\lambda_{\rm n}$ and $A_{\rm Core} = 2\pi Ra$ are the effective areas for the SOL region and core region, respectively. The effective area for the pumping effect is not considered in this paper.

In the C-S-D model, $\lambda_{\rm E}$, λ_Γ are important parameters associated with the radial temperature decay length $\lambda_{\rm T}$ and the radial density decay length $\lambda_{\rm n}$. Since EAST SOL performance for $\lambda_{\rm T}$ and $\lambda_{\rm n}$ cannot yet be reliably predicted from theory, $\lambda_{\rm T}$ can be based on the characteristics of present tokamaks. As an example, in the high temperature regime, i.e. $T_{\rm e-sep} > 40\sim50$ eV, in which $\lambda_{\rm T}$ varies only moderately, the order of magnitude of $\lambda_{\rm T}$ may be estimated by the relationship $\lambda_{\rm T}({\rm m}) = 112R({\rm mag})^{1.21\pm0.04}I_{\rm p}({\rm A})^{-0.69\pm0.03}$ [22]. $\lambda_{\rm n}$ can be obtained from $\Gamma_{\rm sep} = \frac{D}{\lambda_{\rm n}}n_{\rm u}$, where D is the radial particle diffusivity coefficient which is chosen as $D = 0.1\ {\rm m}^2{\cdot}{\rm s}^{-1}$, as compared with the neoclassical value and other tokamak results such as AUG H-mode results [20]. Then $\lambda_{\rm E}$ and λ_Γ can be obtained from relations $\lambda_{\rm E}^{-1} = \lambda_{\rm n}^{-1} + \lambda_{\rm T}^{-1}$ and $\lambda_\Gamma^{-1} = \lambda_{\rm n}^{-1} + (2\lambda_{\rm T})^{-1}$ [23].

3 Calculation results and discussion

In our C-S-D model, $< n >$ and the total input power $Q_{\rm in}$, which are easily controlled or obtained from experiments, are used as the major input parameters and are varied systematically in the calculation to reproduce various operating conditions. The total energy flux from the core across the separatrix is assumed to be 80% of the total input power and the in-out asymmetry caused by the geometry is seen as $\frac{1-\varepsilon}{1+\varepsilon}$ with ε the inverse aspect ratio [20]. With the expansion coefficient $f_{\rm exp}$, the flux expansion at the divertor target is also considered [1,3,20]. Based on the present EAST experiments, $\tau_{\rm E} = f_{\rm H}\tau_{\rm E}^{\rm ITER89P}$ where the confinement improvement factor $f_{\rm H} = 1.5$ for the present LHCD plasmas and the scaling law of the L-mode energy confinement time $\tau_{\rm E}^{\rm ITER89P}$, which agrees with the LHCD experiments, are adopted [7−10]. For $\tau_{\rm p}$, it is assumed that $\tau_{\rm p} = \tau_{\rm E}$ in this paper.

3.1 Comparison of C-S-D model with EAST experiment results

To check the validity of the C-S-D model for H-mode discharge in EAST with the LHCD, a comparison with EAST experiments for shot #32924 is carried out. Shot #32924 is a typical lower single-null H-mode plasma discharge with the LHCD in EAST. The main plasma parameters of shot #32924 and for the C-S-D model are shown in Table 1. The comparison of the C-S-D model with experiment results is listed in Table 2.

Table 1. The main parameters of the C-S-D model and EAST experiment results (shot #32924)

Parameters	Model	Experiment [9]
R (m)	1.9	∼1.9
a (m)	0.5	∼0.5
κ	1.7	∼1.7
$V_{\rm p}$ (m^3)	11.2	∼11.2
$I_{\rm p}$ (MA)	0.63	∼0.63
$B_{\rm T}$ (T)	1.7	1.7
$f_{\rm exp}$	4.1	4.1
$< n > (10^{19}$ m$^{-3})$	2.5	2.5-2.8
$Q_{\rm in}$ (MW)	0.9	∼0.9

Table 2. Comparison of the C-S-D model with EAST experiment results (shot #32924)

Parameters	Model	Experiment [9]
λ_Γ (m)	0.006	∼ 0.008
λ_q (m)	0.005	∼ 0.007
$\Gamma_{\rm T}$ (10^{23} m$^{-2}{\cdot}$s^{-1})	8.4	∼ 7.2
$q_{\rm T}$ (MW$\cdot$m^{-2})	1.07	∼ 0.9 (IR)
		∼ 0.65 (Probe)

From Table 2, we can see that λ_Γ and λ_q obtained from the C-S-D model are smaller while $\Gamma_{\rm T}$ and $q_{\rm T}$ are larger than those obtained from experiments. Especially, $q_{\rm T}$ is almost twice as large as that obtained by the Langmuir probe in the experiment, though it is similar to the result obtained by the IR camera. One of the reasons for the discrepancy between the modeling and the experiment is that the C-S-D model is not sufficient to study the detailed structure of the divertor plasma. As an example, by the improved neutral ionization with the vertical targets adopted in the EAST divertor, the profile of the peak heat flux is broadened [1,2] and the resulting λ_q obtained from the experiments is larger

than that obtained from the C-S-D model. Hence, $q_{\rm T}$ is smaller than that obtained from the C-S-D model because of the total energy conservation. However, in SOL-Divertor plasma simulations, it is usually considered as a good agreement if the discrepancy between the simulation and the experiment is within a factor of 2 [24]. In this sense, Table 2 indicates that the results obtained from the C-S-D model are in good agreement with the experimental results. From the comparison, it is revealed that the results by the C-S-D model are reasonable in a qualitative sense, and it is shown that the C-S-D model is qualified to qualitatively discuss the operation window for EAST.

3.2 Application of the C-S-D model to estimate the EAST operation window

The predictive operation window in a tokamak may provide a reference for the safe operation. The operating window is considered the physics constraints and technical constraints imposed by the divertor system. For EAST, the LHCD is one of the important auxiliary power sources to sustain over 1000 s discharge and can affect the operation window. Therefore, to estimate EAST operation window with the LHCD, we take into account four trade-offs, including the two usual limits: **a.** allowable to the heat load on the divertor plates $q_{\rm T,max} \leq 3.5$ MW·m^{-2} to ensure the energy flux load onto the divertor target below the engineering design maximum [1], **b.** the input power must exceed the L-H transition power for the core plasma to operate in H-mode, and two additional limits associated with the LHCD, **c.** the available LHCD power $P_{\rm LHCD} \leq 4$ MW and **d.** the allowable core density $< n > < 6.0 \times 10^{19}$ m^{-3}, on the assumption that it is not taken into account the FTU method for enabling the LHCD at a high plasma density [16].

Using the EAST engineering design parameters listed in Table 3, the possible operation window in the ($< n >$, $Q_{\rm in}$) plane is shown in Fig. 1. The upper boundary of $< n >$ is dominated by the threshold power $P_{\rm thr}$ ($< n > < 3.6 \times 10^{19}$ m^{-3}) and the available LHCD power $P_{\rm LHCD}$ ($< n > > 3.6 \times 10^{19}$ m^{-3}). For low $Q_{\rm in}$, it requires high $< n >$ to achieve the H-mode. When $< n >$ is up to a certain value ($\approx 3.6 \times 10^{19}$ m^{-3}), it is limited by the amount of $P_{\rm LHCD}$ and by the physics effects at the edge that $< n >$ should be reduced in order to enable penetration of the coupled power to the core [16]. The upper boundary of $Q_{\rm in}$ limited by $q_{\rm T,max}$ is less than 5.45 MW. With increasing $< n >$, the available maximum $Q_{\rm in}$ becomes smaller since $q_{\rm T,max} = \gamma n_{\rm T} V_{\rm T} T_{\rm T} \propto n_{\rm T}$. In the near future, up to 10 MW of input power will be achieved and used to drive over 1000 s in EAST. Therefore, the operation window must be extended to ensure the high input power operation. From Fig. 1, it is indicated that the allowable energy flux load onto the target plate is a key parameter for extending the feasible operation window.

Table 3. The EAST major parameters for comparison between experiments and predictive operation window [1]

Parameters	Value
R (m)	1.97
a (m)	0.5
κ	1.68
$V_{\rm p}$ (m^3)	11.2
$B_{\rm T}$ (T)	3.5
$I_{\rm p}$ (MA)	1.0
$f_{\rm exp}$	5.2 [9]

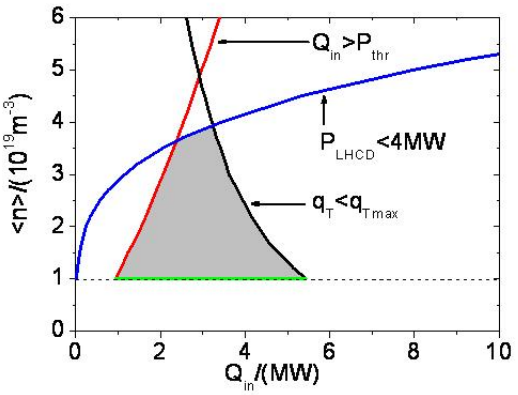

Fig.1 Feature of EAST operation window with LHCD for $I_{\rm LHCD}/I_{\rm p}$=50%

To reduce the energy flux load onto the target plates, gas puffing and impurity seeding have been carried out in EAST experiments and good results have been achieved [6]. It means that gas puffing and impurity seeding can be considered as two effective methods to extend the operation window toward a higher input power. The effects of two candidates on the operation window are shown in Fig. 2(a) and (b). When $N_{\rm puff} = 1.0 \times 10^{21}$ s^{-1} (which is similar to the present EAST experiments [6]) is fuelled into the divertor region, the operation space is extended toward a higher $Q_{\rm in}$. Especially, for a lower $< n >$, the available maximum $Q_{\rm in}$ is extended obviously. As an example, $< n >= 1.0 \times 10^{19}$ m^{-3}, before gas puffing, the available maximum $Q_{\rm in} = 5.45$ MW, while after gas puffing, the available maximum $Q_{\rm in} = 6.48$ MW. However, the extended operation window is not adequate for the up to 10 MW input power. As shown in Ref. [6], a significant reduction of about 50%-70% in the energy flux near the strike point can be seen when the argon (impurity seeding) and its mixture with deuterium are injected into the EAST divertor region. Therefore, we consider the combined effects of impurity seeding and gas puffing on the operation window. With impurity seeding and gas puffing together, similar to the ITER divertor design, when it is possible to increase up to $f_{\rm imp} = 0.5$ of impurity radiation loss fraction [20], then the extended operation window in the ($< n >$, $Q_{\rm in}$) plane is pronounced (Fig. 2(b)). For example, the upper boundary of $Q_{\rm in}$ is extended up to $Q_{\rm in} \approx 9.5$ MW

for $< n >= 1.0 \times 10^{-19}$ m^{-3}. With increasing $< n >$, the available maximum $Q_{\rm in}$ limited by $q_{\rm max}$ decreases, but the operation window is still extended obviously compared with the case shown in Fig. 2(a). As an example, $< n >= 4.0 \times 10^{-19}$ m^{-3}, $Q_{\rm in} \approx 3.61$ MW in the case shown in Fig. 2(a) while $Q_{\rm in} \approx 5.24$ MW in the case shown in Fig. 2(b). It is indicated that impurity seeding is one of the very effective methods to reduce the energy flux to the target plates. Here, it should be pointed out that $f_{\rm imp}$ is given as input parameters in the C-S-D model. The impact of impurity seeding on the core plasma performance should be carefully checked according to the EAST experiments [6]. Examples are the contamination of the core plasma during the impurity seeding. However, by using the C-S-D model, it is revealed that impurity seeding is one of the effective methods to extend the operation window toward higher $Q_{\rm in}$.

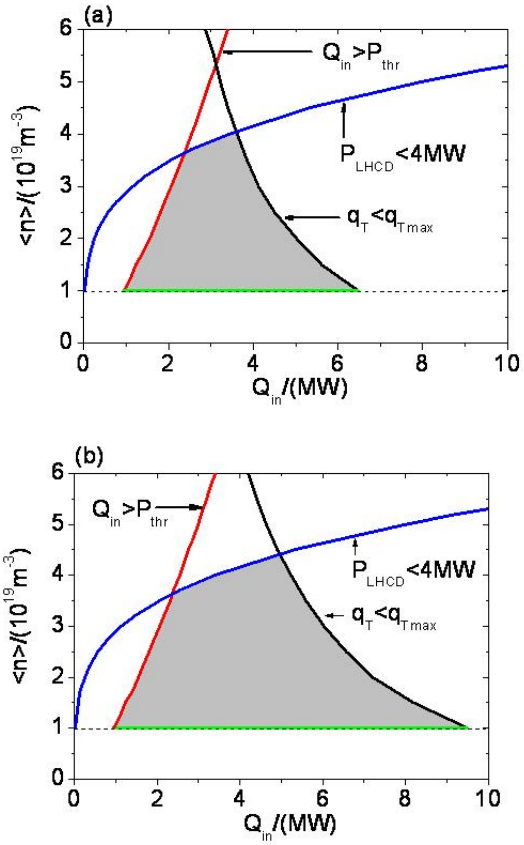

Fig.2 Effect of gas puffing (a) and joint effect of gas puffing and impurity seeding (b) on the EAST operation window with LHCD for $I_{\rm LHCD}/I_{\rm p}$=50%

It is shown in Fig. 1 that the available $P_{\rm LHCD}$ limits the operation window for high $< n >$. Since $P_{\rm LHCD}$ is affected by $I_{\rm LHCD}$ according to Eq. (3), the decreased $I_{\rm LHCD}$ may extend the operation window toward higher $< n >$. The total plasma current $I_{\rm p}$ of EAST engineering design is up to 1 MA, including the Ohmic current, bootstrap current, NBI current and radio-frequency (RF) current. In present EAST experiments, the fraction of the bootstrap current to the total plasma current is only 10% and it is expected to rise to 40% in the future. The increase in the fraction of other currents such as the bootstrap current is one of the methods to decrease $I_{\rm LHCD}$. Fig. 3 shows the operation window for the case of $I_{\rm LHCD}/I_{\rm p} = 30\%$. Compared with the case of $I_{\rm LHCD}/I_{\rm p} = 50\%$ shown in Fig. 2(b), the upper boundaries of the LHCD and the power balance requirement move to a higher density region. Then the boundary of the L-H transition condition limits the operation window at the low input power end: $Q_{\rm in} < 3.0$ MW.

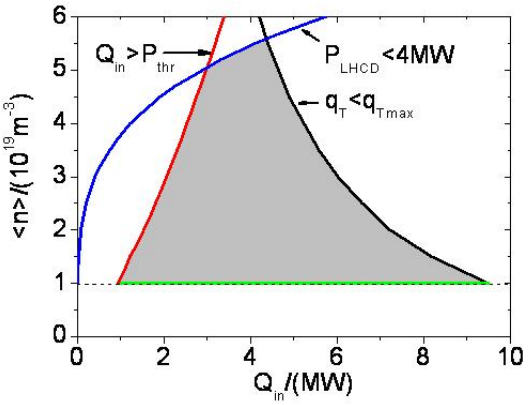

Fig.3 EAST operation window with LHCD for $I_{\rm LHCD}/I_{\rm p}$=30% in the case with gas puffing and impurity seeding together

4 Summary

An operation window for EAST with the LHCD is estimated based on consistent C-S-D modeling in which the core plasma transport and the S-D plasma transport are described by a simple core plasma model of ITER physics guidelines and a two-point model, respectively. The C-S-D model is validated by the present EAST divertor experiments. Based on a number of limits, including the two usual limits, **a.** the allowable heat load onto the divertor plates and **b.** the threshold power for L-H transition, and two additional limits associated with the LHCD, which impose significant constraints to the operation window, i.e. **c.** the available LHCD power and **d.** the allowable core density during LHCD, the operation window of EAST in H-mode operation has been determined by a systematic variation of the line average density and input power. Our numerical results show that the maximum allowable energy flux to the target plates limits the increase in the input power. To extend the operation window for high input power, gas puffing and impurity seeding are considered as two effective methods. However, the effect of the gas puffing on the extended operation window is not adequate for the up to 10 MW input power. The impurity seeding is a very effective method to extend the operation window, but it may have influence on the core plasma performance. In addition, the operation window moves to a high density region with the decrease in the LHCD current. The description of the operation window provides a reference for the EAST experiments with a LHCD in the future to ensure energy

flux load onto the divertor target below the engineering design maximum and maintain core plasma in H-mode. However, for the high plasma density, the FTU method should be utilized to enhance the LHCD effect by means of operations which produce relatively high electron temperature in plasma edge and periphery [16]. Finally, note that the present C-S-D model can only make some qualitative predictions about the EAST operation window. To further investigate the EAST operation window, a C-S-D plasma simulation with a 1.5-D code such as ONETWO for the core plasma and a 2-D code such as B2-EIRINE for the SOL and divertor plasma will be carried out in future.

References

1 Zhu S. 2000, Contrib. Plasma Phys., 40: 322
2 Zhu S, Hiwatari R, Hatayma A A, Tomita R. 2006, Plasma Sci. Technol., 8: 118
3 Jin L, Zhu S. 2007, Plasma Sci. Technol., 9: 403
4 Hiwatari R, Kuzuyama Y, Hatayama A, et al. 2005, J. Nucl. Mater., 337: 386
5 Hiwatari R, Hatayama Y, Zhu S, Tomita Y. 2009, Plasma Sci. Technol., 11: 389
6 Wang D S, Guo H Y, Wang H Q, et al. 2011, Phys. Plasmas, 18: 032505
7 Yang Y, Gao X, EAST team. 2011, Plasma Sci. Technol., 13: 312
8 Li M H, Ding B J, Kong E H, et al. 2011, Chin. Phys. B, 20: 125202
9 Wang L, Xu G S, Guo H Y, et al. 2012, Nucl. Fusion, 52: 063024
10 Liu Z X, Gao X, Zhang W Y, et al. 2012, Plasma Phys. Control. Fusion, 54: 085005
11 Pacher G W, Pacher H D, Janeschitz G, et al. 2004, Plasma Phys. Control. Fusion, 46: A257
12 Pacher G W, Pacher H D, Janeschitz G, et al. 2008, Nucl. Fusion, 48: 105003
13 Stankiewica R and Zagórski R. 2001. J. Nucl. Mater., 290: 738
14 Zhou D, Holger S J, Hu Y M, et al. 2009, Plasma Sci. Technol., 11: 417
15 Uchan N and ITER Physics Group. 1990, ITER Physics Design Guidelines: 1989 ITER Documentation Series No. 10
16 Cesario R, Amicucci L, Cardinali A, et al. 2010, Nature Comms., 1: 55
17 Martin Y R, Takizuka T, ITPA CDBM H-mode Threshold Database Working Group. 2008, J. Phys.: Conf. Ser., 123: 012033
18 Ou J, Yang J H. 2011, Chin. Phys. B, 20: 095201
19 Ou J, Yang J H. 2012, Acta Phys. Sin., 61: 075201 (in Chinese)
20 Pitcher C S, Stangeby P C. 1997, Plasma Phys. Control. Fusion, 39: 779
21 Miyamoto K, Asakura N. 1988, J. Plasma Fusion Res., 74: 266
22 ITER Physics Expert Group on Divertor. 1999, Nucl. Fusion, 39: 2391
23 Stangeby P C. 2000, The Plasma Boundary of Magnetic Fusion Devices. Bristol, Institute of Plasma Publishing, UK, p.602
24 Kotov V, Reiter D, Pitts R A, et al. 2008, Plasma Phys. Control. Fusion, 50: 105012

(Manuscript received 19 August 2013)
(Manuscript accepted 5 March 2014)
E-mail address of OU Jing: ouj@ipp.ac.cn